THE OPHIOLITE-BEARING MÉLANGE IN THE EARLY TERTIARY PINDOS FLYSCH OF ETOLIA (CENTRAL GREECE)

Valerio Bortolotti*,✉, Nicola Carras **, Marco Chiari*, Milvio Fazzuoli*, Marta Marcucci***, Giuseppe Nirta*, Gianfranco Principi*,*** and Emilio Saccani°**

   * *Dipartimento di Scienze della Terra, Università di Firenze, Italy.*
 ** *Institute of Geology and Mineral Exploration (IGME), Greece.*
*** *C.N.R., Istituto di Geoscienze e Georisorse, U.O. di Firenze, Italy.*
  ° *Dipartimento di Scienze della Terra, Università di Ferrara, Italy.*
 ✉ *Corresponding author, e-mail: valerio.bortolotti@geo.unifi.it*

ABSTRACT

In Etolia (Central Greece), west of the Parnassus/Vardoussia units, the Pindos succession crops out, with its higher formation: the Pindos Flysch. In its upper portion levels of debris flow deposits and slide blocks (olistostromes and olistoliths) contain ophiolitic material with fragments derived from the Parnassus/Vardussia formations.

This ophiolitic material consists of serpentinites, basalts of WPB, E- and N-MOR affinity, and radiolarian cherts of Middle-Late Triassic and Middle-Late Jurassic age. Petrologic and biostratigraphic analyses confirm that the mélange has the same features of the sub-ophiolitic mélanges present at the base of the ophiolitic masses in Greece. Linked to the flysch, with contacts of unclear nature, a rhyolites body of Middle Triassic age indicates the continental nature of the Pindos Basin. In fact, here, as all over the Albanian-Greek section of the Dinarides, no record of an oceanic area in the central portion of the Dinarides exists: the Parnassus and Vardoussia units were directly thrust onto the Pindos Basin.

The intercalations of ophiolitic and continent-derived material in the flysch, are interpreted as the forerunners of the Ophiolitie Nappe which, coming from the Vardar Ocean located to the east, reached during the Eocene the Pindos Basin.

INTRODUCTION

This paper presents new biostratigraphic, geochemical and field data on some ophiolites (basalts and overlying cherts) present as slide blocks and debris flow deposits (mélange Auctt.) included in the Eocene Pindos Flysch of east Etolia. New biostratigraphic and geochemical data are also presented on an outcrop of Triassic volcanics and cherts intercalated, probably as a tectonic slice, in the same Pindos Flysch.

The results give us the opportunity to discuss the relationships of these ophiolites with the Ophiolitic Unit cropping out all along the Dinaric-Hellenic chain (in particular with the Othris Massif, the nearer ophiolites, on the eastern side of the Parnassus, see Bortolotti et al., 2008) and to stress their importance; as they testify the foremost outcrops of the Ophiolitie Nappe in its long thrust journey from the Vardar Ocean toward the west.

GEOLOGICAL SETTING

In Central Greece, the eastern margin of the Adria Plate is represented by a west-verging pile of tectonic units. From west to east and from the bottom to top this nappe pile includes the following main units: 1- Ionian, 2- Gavrovo-Tripolitsa, 3- Pindos; 4- Parnassus and, 5- Pelagonian, here considered as the easternmost portion of the plate margin. At the top of the pile, the Ophiolite Nappe along with an underlying ophiolitic mélange crops out in the Mt. Iti and Kallidromon area (Karipi et al., 2008).

In eastern Etolia, (Fig. 1) three main tectonic units crop out: piled up from east to west. From east to west and from the top downwards they are: **a**- some *klippen* of the Pelagonian Unit with a succession similar to that of the underlying **b**- the Parnassus Unit, consisting of a persistent carbonatic platform of Triassic to Cretaceous age, covered by Paleocene marlstones and an Eocene flysch; **c**- the Vardoussia Unit, corresponding to the Cretaceous western slope of the Parnassus succession, toward the Pindos Basin, and consisting of pelagic sediments with intercalations of debris flows and slide blocks coming from the Parnassus platform; **d**- the Pindos Unit, matter of the article, consisting of a Mesozoic continental margin succession, which includes deep water carbonates, radiolarites and shales, covered by a Paleocene-Eocene syn-orogenic flysch, the Pindos Flysch (Richter and Mueller, 1993; Neumann et al., 1996; Degnan and Robertson, 1998). The Pindos Flysch consists of fine-grained and thin bedded sandstones alternating with shales, and with sporadic conglomerate lenses. Arenites show a lithoarenitic composition (Dickinson and Suczek, 1979) reflecting a source area from a "recycled" orogenic wedge (Gonzales-Bonorino, 1996). Sedimentologic studies, the interpretation of paleocurrents, (British Petroleum, 1970; Piper et al., 1978; Alexander et al., 1990; Richter et al., 1978; Leigh, 1991) and petrographic analyses (Gonzales-Bonorino, 1996; Faulp et al., 1999; 2002; Vakalas et al., 2004) indicate for the Pindos Flysch a provenance from an orogenic wedge located to the east. In particular lithic fragments in the Flysch derived from metamorphic rocks, limestone, basalt, chert and serpentinite testify both continental and oceanic source terrains.

Along the north-south trending fold-and thrust structure on the western side of the Vardoussia Mountains, between Milia and Artotina, the Pindos Flysch also includes levels of debris flow deposits and slide blocks (as in the Pindos Massif area,
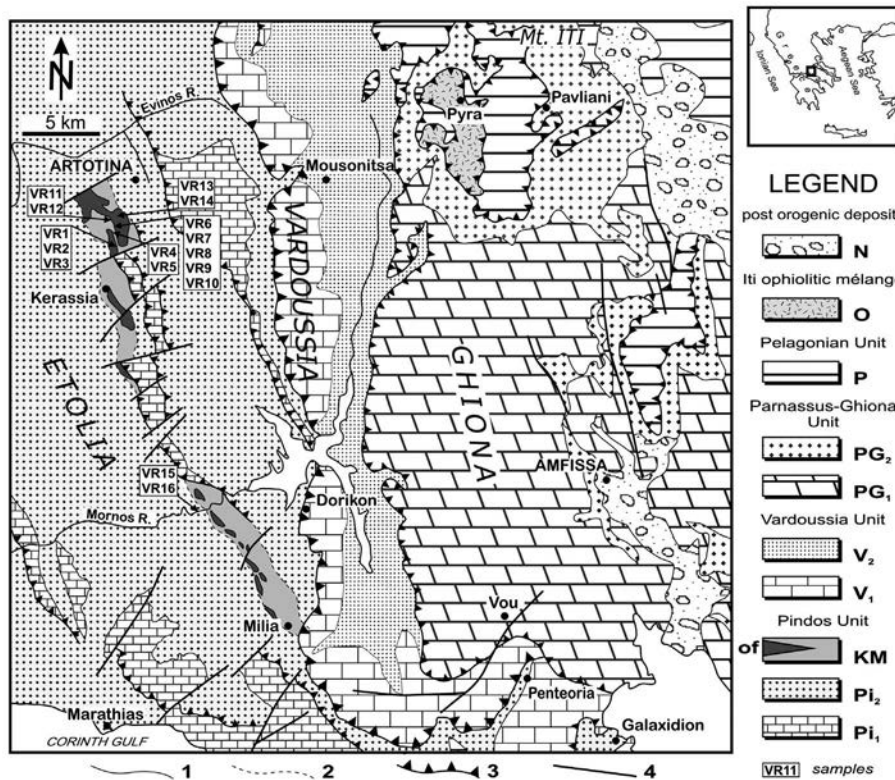
Fig. 1 - Geological and structural sketch map of east Etolia-Ghiona area. N- Neogene - Quaternary late orogenic deposits. O- Iti ophiolitic mélange. Pelagonian Unit: P- Triassic-Kimmeridgian carbonate sequence. Parnassus Unit: PG_2- Eocene flysch; PG_1- Triassic - Upper Cretaceous carbonate sequence. Vardoussia Unit: V_2- Eocene Flysch; V_1- Mesozoic carbonate and siliceous sequence. Pindos Unit: KM- small scale slide blocks and debris flow deposits, of- ophiolitic slide blocks; Pi_2- Paleocene-Eocene Flysch; Pi_1- Mesozoic carbonate and siliceous sequence. 1- stratigraphic contact; 2- presumed stratigraphic contact; 3- thrust; 4- fault. Modified after Celet (1977) and Beck (1980).

see Principi et al., 2008, Nirta et al., 2009) mainly comprising fragments of ocean-derived material (basalts, at places covered by red ribbon cherts, ophiolitic sandstones, andesites, serpentinites and gabbros) and in lesser amount, of continent-derived material (pelagic ammonite-bearing limestones, neritic limestones with *Megalodon*, marls, cherty- and clay-pelites, sometimes alternating with thin platy limestones of Malm age).

The smaller ophiolitic blocks (metric to hectometric) and their matrix are clearly included as debris flow deposits and slide blocks into the Pindos Flysch, while the larger blocks have not always clear relationships with the flysch, due to successive tectonic movements. However, the presence of ophiolite bearing debris flow deposits closely associated with the huge blocks permits to consider also these latter as slide blocks (Beck, 1980).

Is noteworthy to give some hint to the previous works dealing with this mélange.

Since 1962, Celet noted that in Etolia the Eocene Pindos Flysch included *"des enclaves basiques",* and that *"étant donnée la distance qui les sépare des formations éruptives charriées de l'Iti, il se pourrait qu'il s'agisse de lambeaux détachés du complex ophiolitique et glissés sur le fond [...] de la mer éocène lors du dépôt du Flysch"* Celet, 1962, p. 104). This intuition, basically stating the presence of slide blocks included in the flysch, was confirmed later on by the same author (e.g., Celet, 1977, Discussion) referring to the Thesis of Beck (1975). This author (Beck, 1980) assumes that the ophiolitic material (olistostromes and olistoliths) derived from the "Pelagonian Nappe" an allochthonous unit containing some ophiolite masses, coming from the east of the "Parnassus Zone".

Afterwards, Robertson et al. (1991), Robertson and Degnan (1993) and Pe-Piper and Hatzipanagiotou (1993) dealing in particular with the Kerassia-Milia Complex (the ophiolite-bearing mélange sandwiched in the Pindos Flysch), proposed the idea that the ophiolitic material included in the Pindos

succession from the Late Cretaceous to the Eocene, formed entirely within the Pindos Ocean. In the Robertson and Degnan (1993) reconstruction, the Parnassus carbonate platform would be a continental block completely surrounded by oceanic areas: to the east the Pindos Ocean, to the west a secondary basin of the same Ocean: the Kerassia-Milia Basin. During the Late Cretaceous an extensional event allowed the peridotites to be exposed on the ocean floor. During the Early Tertiary compressive events caused the highs of the oceanic floor to be "accreted into Eocene turbidites" (i.e., the Pindos Flysch) and, successively they caused the closure of the whole Pindos Ocean. A Kerassia small ocean basin, separated from the Pindos Ocean by the Parnassus continental block is hypothesized also by Pe Piper and Piper (2002).

Our field observations, accompanied by petrologic and biostratigraphic analyses allowed us to present a more viable hypothesis which considers the mélange of the Kerassia-Milia zone, as a complex of debris flows and slide blocks of various sizes that glided in the Pindos Flysch basin from the Sub-ophiolitic mélange (see Bortolotti et al., 2004) that lies at the base of the Ophiolite Nappe located to the east (e.g., on the Iti Mt.).

DESCRIPTION OF THE SAMPLED AREAS

Our interest was for the volcanics and related cherts, linked to the flysch, which we sampled in two different settings:

1- the thicker mélange level intercalated in the geometrically higher portion of the Pindos Flysch, cropping out north of the Mornos River, along the road between Kerassia and Artotina, west of the Vardoussia and Ghiona Mts. This level yielded chert and basalt samples (Fig. 1): 7 basalts for geochemistry and 7 radiolarian cherts for biostratigraphy, that come from five outcrops, starting at the crossroads toward Kriatsi and Kalloni and going up to the north. This mélange
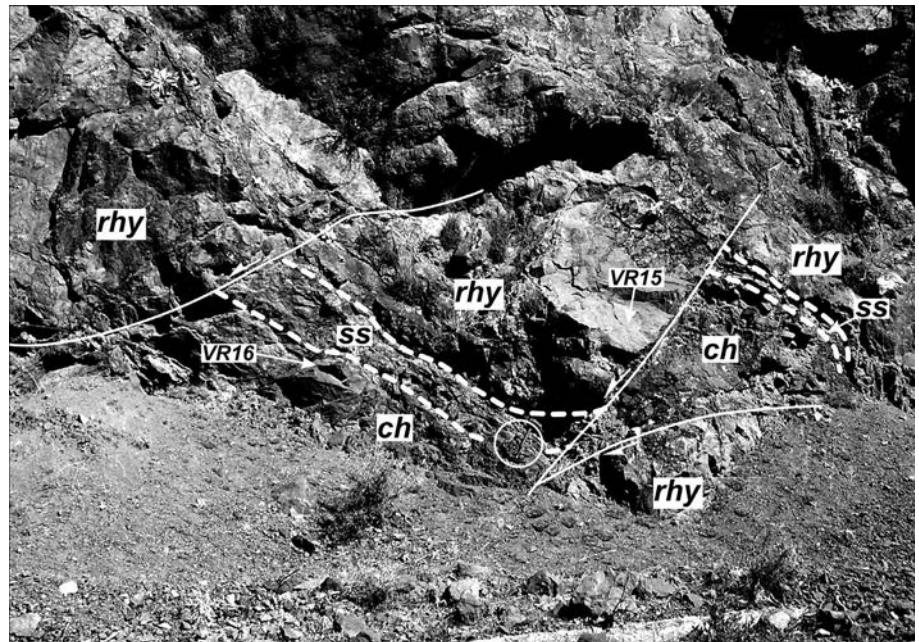
Fig. 2 - Rhyolite - cherts contact at outcrop 6. rhy: rhyolite; ss: greenish sandstones; ch: cherts; VR15, VR16: sampling sites.

is an assemblage of debris flow deposits, which comprises slide blocks of various compositions and sizes: basic and ultrabasic rocks, cherts, pelagic and neritic limestones, marlstones, and shales.

2- Two other samples (1 volcanic rock for geochemistry and 1 radiolarian chert for biostratigraphy) were collected on the road running along the Mornos River, between the km 134 and 135 (Samples VR15 and VR16 in Fig. 1) from an outcrop consisting of, from bottom upwards: a- a very thick block (not less than 100 m) made of an overturned sequence of volcanics covered by about 20 cm of greenish arenites grading to 1 m of red cherts, b- fragmented whitish limestones, c- whitish and pink limestones with red shales (Fig. 2).

SAMPLING

a- Road Kerassia - Artotina

Outcrop n. 1, crossroads toward Kriatsi and Kalloni (N38°39.520', E022°01.269').

The outcrop consists of blocks of sepentinites, tectonically juxtaposed to basalts and cherts, without evidences of a stratigraphic succession.

The basalt VR2 shows a WPB affinity, the radiolarian cherts, VR1 and VR3 collected in two different blocks yielded, respectively, radiolarian assemblages of late Bathonian-early Callovian to middle Callovian-early Oxfordian (Middle-Late Jurassic) and latest Anisian (late Illyrian, Middle Triassic), after the definition of Anisian/Ladinian boundary, in Brack et al. (2005).

Outcrop n. 2, about 1650 m to the north (N38°40.127', E022°01.029').

The outcrop consists of blocks of pillow basalts including boudins of cherts and of whitish and pinky bedded limestones, alternating with red marls and limestones.

The basalt VR4 is of WPB affinity, the manganiferous chert VR5 yielded a radiolarian assemblage of late Anisian (Middle Triassic) after the definition of Anisian/Ladinian boundary, in Brack et al. (2005).

Outcrop n. 3, about 150 m to the north (N38°40.248', E022°01.065').

The outcrop consists of blocks of sheared serpentinite, reddish limestones and basalts stratigraphically covered by some meters of disrupted radiolarian cherts. The basalts VR6 and VR10 are sampled at the contact with the cherts VR7. The basalt VR9 and the chert VR8 are of uncertain stratigraphic position.

The basalts VR6 and VR9 resulted of E-MOR affinity, the VR10 of N-MOR affinity, the chert VR7 yielded a radiolarian assemblage of latest Carnian-early Norian (Late Triassic). The sample VR8 yielded very poor preserved radiolarians.

Outcrop n. 4, about 135 m to the north (N38°40.371', E022°01.022').

The outcrop consists of blocks of pillow basalts and manganiferous cherts without evidences of stratigraphic relationships and of red shales including fragments of whitish and pinky limestones.

The basalt VR11 is of WPB affinity, the chert VR12 yielded a radiolarian assemblage of early-middle Bajocian to middle Callovian-early Oxfordian (Middle-Late Jurassic).

Outcrop n. 5, about 250 m to the north (N38°40.472', E022°01.146')

The outcrop consists of blocks of sheared serpentinites, basalts with cherts, reddish limestones and marls. The pillow basalts are strongly altered and deformed and include, among them, large boudins of slightly recrystallized cherts.

The basalt VR13 shows a WPB affinity, the chert VR14 yielded very poor preserved radiolarians.

b- Road along the Mornos River

Outcrop n. 6 (N38°30.806', E022°04.571')

The outcrop, between the km 134 and 135, consists of an overturned block of volcanics stratigrafically covered by about 20 cm of greenish arenites grading to red cherts (Fig. 2).

The volcanic rock VR15 resulted a rhyolites, the chert VR16 yielded a radiolarian assemblage late Anisian (early Illyrian, Middle Triassic), after the definition of Anisian/Ladinian boundary, in Brack et al. (2005).

PETROGRAPHY, GEOCHEMISTRY AND TECTONO-MAGMATIC SIGNIFICANCE OF VOLCANIC ROCKS

Petrography

All samples are affected by variable degrees of ocean-floor hydrothermal alteration under static conditions. This alteration has generally resulted in re-crystallization of the primary igneous phases. Commonly, plagioclase is replaced by albite + calcite or albite + epidote; clinopyroxene is replaced by amphibole and/or chlorite; volcanic glass is replaced by clay minerals and chlorite. By contrast, the primary igneous textures are well preserved. The petrographic features of the analyzed samples are presented below, according to the four different groups of rock recognized on the basis of the chemical analyses, and described in the next section.

Group 1: alkaline basalts. These basalts range in textures from aphyric to slightly porphyritic (PI ~15%). In the porphyritic varieties, microphenocrysts are represented by very altered plagioclase and relatively fresh clinopyroxene set in a microcrystalline groundmass showing ophitic texture. In the aphyric rocks, textures are generally ophitic and hyalophitic with variable grain size, ranging from microcristalline to scarse-grained doleritic. Mineral assemblages include plagioclase, clinopyroxene and, locally opaque minerals.

Group 2 and Group 3: mid-ocean ridge basalts. They show textures including very fine-grained aphyric varieties with sub-ophitic groundmass and coarse-grained aphyric types. Both are characterized by euhedral plagioclase and anhedral to interstitial clinopyroxene. Such a texture testifies for the early crystallization of plagioclase with respect to clinopyroxene. Basalt VR6 shows significant amounts of opaque minerals, while basalt VR9 is characterized by abundant chlorite veins.

Group 4: calc-alkaline rhyolite. This rock (sample VR15) displays slightly porphyritic, vitrophiric texture, where the volcanic glass is totally replaced by a very fine-grained (cryptocrystalline) assemblage of chlorite and clay minerals. Aggregates of secondary minerals most likely pseudomorph after microphenocrysts of plagioclase are also observed.

Analytical methods

Bulk-rock major and some trace (Zn, Cy, Sc, Ga, Ni, Co, Cr, V, Rb, Ba, Sr, Zr, Y, La) element analyses were performed by X-ray fluorescence spectrometry (XRF) on pressed powder pellets with an ARL Advant-XP automated spectrometer. The matrix correction methods proposed by Lachance and Trail (1966) were applied. Rare earth elements (REE), Rb, Hf, Ta, Th, U, Nb, Sr, Zr, and Y were determined by inductively coupled plasma-mass spectrometry (ICP-MS) using a VG Elemental Plasma Quad PQ2 Plus spectrometer. Accuracy and detection limits were determined using a set of international standards for both XRF and ICP-MS analyses. Accuracy for XRF analyses is better than 3% for Si, Ti, Ca, K and 7% for Al, Mn, Mg, Na, P, and better than 6% for trace elements, with the exception of Ba (8%), Th (10%), and Nb (13%). Detection limits for trace elements are: Zn, Cu, Sc, Ba = 5 ppm; Ga, Ni, Co, Cr, V, Nb, La, Sr, Zr, Y = 2 ppm; Th, Rb = 1 ppm. Accuracy for ICP-MS analyses ranges from 2 to 7 relative percent, with the exception of Nb (12%), Ta (16%), and U (9%). Detection limits are: Nb, Hf, Ta = 0.02 ppm; Th, U = 0.01 ppm; light (L-) and medium (M-) rare earth elements (REE)

< 0.07 ppm; heavy REE (HREE) < 0.13 ppm.

Volatiles were determined as loss on ignition (L.O.I.) at 1000°C. All analyses were performed at the Department of Earth Sciences of the University of Ferrara. Chemical compositions are presented in Table 1.

Geochemistry and tectono-magmatic interpretation

The petrographic analyses indicate that most of the samples underwent ocean-floor hydrothermal processes. It is well-known that these processes commonly result in variable mobilization of large ion lithophile elements (LILE), such as Ba, Rb, K, and Sr, whereas the transition metals (V, Cr, Mn, Fe, Co, Ni, Zn) and high field strength elements (HFSE) (Zr, Y, Nb, Ti, Hf, P) are relatively immobile, and largely reflect primary, magmatic abundance (Pearce and Norry, 1979; Shervais, 1982; Pearce, 1983). REE are also thought to be relative immobile during alteration processes, although LREE may be slightly mobile when compared to HREE. The co-variations of Rb, Ba, K, and Sr with respect some HFSE (not shown) indicate that these elements have been largely mobilized in the studied volcanic rocks. By contrast, Th, Ta, and, to a lesser extent U, plotted against HFSE (not shown) indicate a scarce mobilization of these elements. For these reasons, the discussion on the geochemical and petrogenetic features of the studied rocks will be mainly based on those elements which can be considered immobile during metamorphic and alteration processes.

The data presented in this paper point out the occurrence of four geochemically distinct groups of lavas in this Etolia mélange.

Group 1 (Alkaline basalts).

Group 1 basalts includes samples VR2, VR4, VR11, VR13, which are representative of outcrops 1, 2, 4, 5, respectively (Fig. 1). The Nb/Y ratios (Table 1) are > 0.70, thus evidencing the transitional to alkaline nature of these rocks. In general, they display quite uniform compositions and likely represent rather primitive or slightly evolved magmatic products, as demonstrated by their relatively high Mg# (66.1-76.2) and MgO (7.37-15.69 wt%) and relatively low SiO_2 (47.35-49.35 wt%) contents. CaO is also generally high (8.06-12.17 wt%), with the only exception of sample VR2 (CaO = 3.25 wt%).

The incompatible element abundances (Fig. 3a) are characterized by regularly decreasing patterns from Th to Yb, as well as by a generalised enrichment in LILE with respect to MORB. The REE patterns (Fig. 3b) display marked LREE enrichment with respect to HREE, exemplified by La_N/Yb_N ratios ranging from 3.31 to 7.40. The overall REE enrichment ranges from ~10 to ~80 times chondrite for Yb and La, respectively. These chemical features are comparable to those of typical within-plate alkaline basalts, such as ocean island basalts (OIBs) (Frey and Clague, 1983; Lipman et al., 1989; Haase and Devey, 1996). This conclusion is supported by the discrimination diagram of Fig. 4, where Group 1 basalts plot in the field for alkaline within-plate basalts.

The geochemistry of Group 1 basalts implies derivation from a mantle source distinct from depleted MORB-type mantle. OIB-like trace element and REE compositions suggest that these rocks represent magma generation associated with a plume-type geochemical component. The Th/Yb vs. Ta/Yb ratios (Fig. 5) and Th/Tb vs. Th/Ta ratios (Fig. 6) indicate that these rocks were generated from an enriched

Table 1 - Bulk rock major and trace element analyses of volcanic rocks from the mélange.

Outcrop	1		2		4		5		3		3		3		6	
Sample	VR2		VR4		VR11		VR13		VR6		VR9		VR10		VR15	
Rock	Bas		Bas		Bas		Bas		Bas		Bas		Bas		Rhy	
Type	WPB		WPB		WPB		WPB		E-MORB		E-MORB		N-MORB		CAB	
	a	b	a	b	a	b	a	b	a	b	a	b	a	b	a	b
SiO_2	47.95		48.33		49.35		47.35		49.17		47.16		50.78		72.52	
TiO_2	1.74		1.61		1.18		0.97		2.13		2.12		1.84		0.47	
Al_2O_3	13.10		12.32		11.93		12.44		14.70		12.09		15.07		11.69	
Fe_2O_3	1.31		1.10		0.91		1.04		1.29		1.09		1.35		0.31	
FeO	8.72		7.30		6.07		6.93		8.61		7.27		9.03		2.06	
MnO	0.30		0.28		0.15		0.14		0.26		0.22		0.20		0.06	
MgO	15.69		12.92		7.37		7.58		7.12		6.81		6.30		3.34	
CaO	3.25		8.06		12.17		11.75		9.36		13.85		9.80		0.94	
Na_2O	2.19		2.16		4.15		2.79		3.55		3.41		3.48		4.77	
K_2O	0.04		0.19		0.64		1.57		0.08		0.18		0.28		2.32	
P_2O_5	0.33		0.27		0.21		0.19		0.36		0.33		0.23		0.12	
L.O.I.	5.38		5.58		5.93		7.32		3.18		5.56		1.58		1.44	
Total	99.99		100.11		100.05		100.07		99.80		100.09		99.95		100.03	
Mg#	76.2		75.9		68.4		66.1		59.6		62.5		55.4		74.3	
Zn	54		61		73		64		90		92		80		15	
Cu	35		26		37		60		73		57		73		n.d.	
Sc	38		25		18		18		38		35		36		9	
Ga	23		16		10		10		28		22		23		8	
Ni	93		44		77		140		60		74		47		3	
Co	44		30		36		42		39		40		41		5	
Cr	278		137		69		302		256		203		136		n.d.	
V	277		270		253		238		319		315		304		45	
Rb	3	2.58	1	1.55	11	12.2	21	23.5	n.d.	0.68	2	1.05	2	1.57	23	22.3
Ba	421		144		100		133		86		96		91		156	
Hf		3.77		4.24		2.62		2.09		5.03		4.78		2.87		3.21
Ta		1.32		1.58		1.46		1.22		0.80		0.96		0.24		0.63
Th	2	1.71	2	2.10	2	1.99	2	1.58	1	0.90	1	1.07	n.d.	0.20	6	5.70
U		0.54		0.66		1.03		0.61		0.30		0.80		0.09		2.36
Nb	18	19.0	20	22.9	19	20.7	15	17.2	9	10.7	12	13.2	3	2.74	6	7.48
Sr	79	79.8	222	221	192	189.7	166	164	181	172	241	242	331	326	39	36.7
Zr	153	145	120	122	80	80.9	58	63.2	171	175	162	168	120	118	77	73.8
Y	27	25.0	32	33.9	22	20.9	20	18.3	36	34.0	40	38.9	35	34.4	25	23.3
La	13	13.3	14	13.2	20	18.2	12	9.3	12	12.6	13	11.0	5	3.12	13	10.4
Ce		29.8		31.9		34.2		21.6		29.0		27.6		11.1		22.3
Pr		4.02		4.37		4.11		2.9		3.63		4.02		1.98		2.74
Nd		16.9		19.0		16.5		12.2		17.0		17.7		10.5		11.0
Sm		4.36		5.14		3.43		3.12		4.54		4.84		3.48		2.42
Eu		1.20		1.46		1.03		0.85		1.46		1.53		1.24		0.44
Gd		3.88		4.65		3.15		2.87		4.61		4.93		4.53		2.21
Tb		0.58		0.75		0.49		0.44		0.78		0.82		0.84		0.38
Dy		3.71		4.93		3.05		2.92		5.21		5.35		4.99		2.27
Ho		0.78		1.06		0.65		0.64		1.10		1.14		1.10		0.47
Er		2.09		2.91		1.75		1.75		2.96		3.06		3.01		1.29
Tm		0.31		0.44		0.26		0.28		0.44		0.45		0.46		0.18
Yb		2.04		2.86		1.77		1.74		2.78		2.91		3.00		1.15
Lu		0.30		0.44		0.27		0.27		0.40		0.43		0.44		0.16
Ti/V	40		38		30		26		41		43		37		64	
Nb/Y		0.70		0.72		0.93		0.85		0.30		0.33		0.08		0.30
Ce/Y		1.09		1.00		1.53		1.07		0.80		0.69		0.31		0.90
$(La/Sm)_N$		1.97		1.66		3.43		1.93		1.79		1.47		0.58		2.78
$(Sm/Yb)_N$		2.37		1.99		2.16		2.00		1.81		1.85		1.29		2.33
$(La/Yb)_N$		4.66		3.31		7.40		3.85		3.23		2.71		0.75		6.48

Location of samples is reported in Fig. 1. Abbreviations: Bas- basalt; Rhy- rhyolite; WPB- within-plate alkaline basalt; E-MORB- enriched-type mid-ocean ridge basalt; N-MORB- normal-type mid-ocean ridge basalt; CAB- calc-alkaline; a- XRF analyses; b- ICP-MS analyses; n.d.- not detected. Fe_2O_3- 0.15 x FeO; Mg#- 100 x Mg/(Mg+Fe^{2+}), where Mg- MgO/40 and Fe- FeO/72. Normalizing values for REE ratios are from Sun and McDonough (1989).
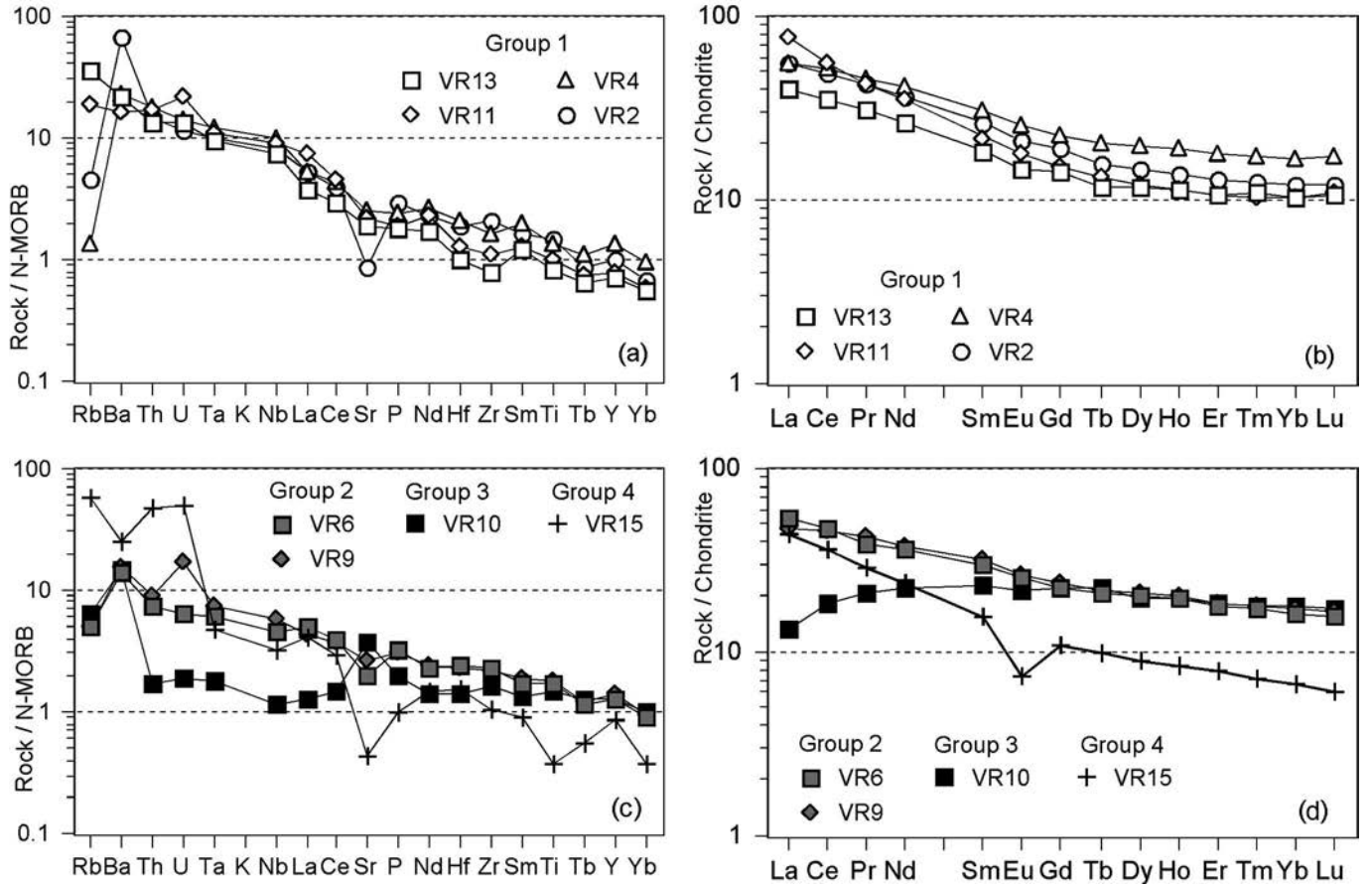
Fig. 3 - a, c: N-MORB normalized incompatible element; b, d: chondrite-normalized REE patterns for volcanic rocks from the mélange. Normalizing values are from Sun and McDonough (1989).
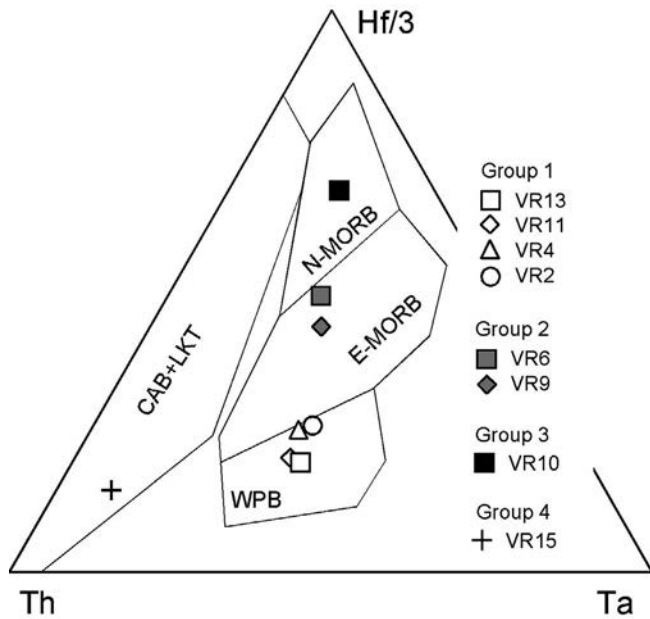

Fig. 4 - Th, Ta, Hf/3 discrimination diagram (Wood, 1980) for volcanic rocks from the mélange. Abbreviations: N-MORB- normal-type mid-ocean ridge basalts; E-MORB- enriched-type mid-ocean ridge basalts; WPB. within-plate alkaline basalts; CAB- calc-alkaline basalts; LKT- low-K tholeiites.
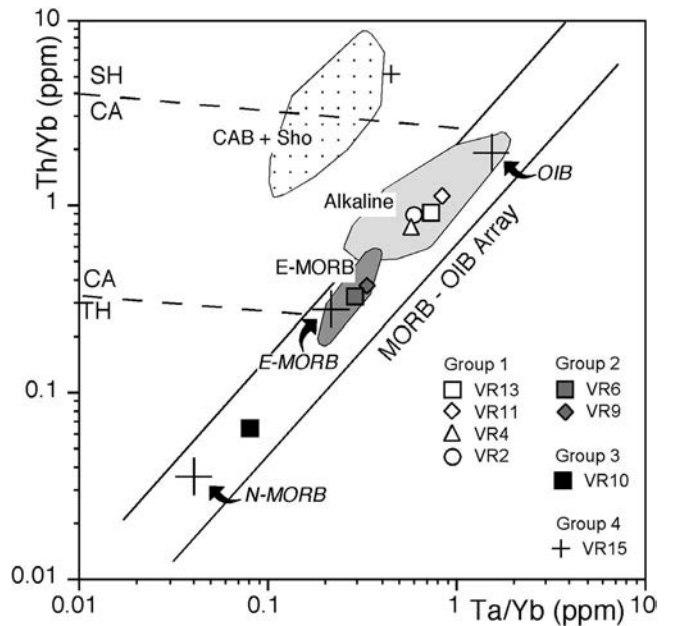

Fig. 5 - Th/Yb vs. Ta/Yb diagram for volcanic rocks from the mélange. Large crosses indicate the compositions of Modern ocean-island basalt (OIB), enriched-type mid-ocean ridge basalt (E-MORB), and normal-type mid-ocean ridge basalt (N-MORB), according to Sun and McDonough (1989). Variations of elemental ratios of Triassic calc-alkaline basalts (dotted field), Triassic alkaline basalts (light gray field), and E-MORBs (dark gray field) from various localities of the Hellenides are reported for comparison (data from Pe-Piper and Piper, 2002; Saccani and Photiades, 2005, and references therein).

mantle-type source without any detectable influence of continental crust contamination. According to the model proposed by Haase and Devey (1996), the $(Dy/Yb)_N$ and $(Ce/Yb)_N$ ratios (Fig. 7) are compatible with low degree (6-8%) partial melting of a theoretical plume-type source. The high $(Ce/Yb)_N$ ratios of sample VR11, when compared with other alkaline basalts, may be related to the slightly evolved nature of this basalt or, alternatively, to a different composition of its mantle source. The REE pattern of this sample, which crosses the patterns of other alkaline basalts suggests that the second alternative is the most appropriate for the genesis of sample VR11.

As exemplified in Fig. 5, the chemistry of these rocks is comparable with that of transitional to alkaline rocks (many of them Triassic in age) included in various sub-ophiolitic mélange units of both the Internal and External Hellenide Ophiolites (Saccani and Photiades, 2005; Saccani et al., 2008). Many authors (e.g., Jones and Robertson, 1991; Pe-Piper, 1998; Saccani et al., 2003a, 2003b, 2008; Saccani and Photiades, 2005) suggested that transitional to alkaline basalts in the Hellenide mélanges originated in intraplate oceanic island settings. Nonetheless, voluminous Lower-Middle Triassic alkali basalts, which are associated to the Permo-Triassic continental rifting of Gondwana are found in the Pelagonian continental margin (e.g., Pe-Piper, 1998). Based on the comparison with the overall geological characteristics of these different Triassic alkaline basalts, it can be postulated that Group 1 alkaline basalts from this Etolia mélange most likely represent seamount material or volcanic rocks erupted at the ocean-continent transition zone.

Group 2 (Enriched-type mid-ocean ridge basalt).

Group 2 basalts are represented by samples VR6 and VR9 from outcrop 3 (Fig. 1). They display a clear sub-alkaline nature, as exemplified by the Nb/Y ratios (Table 1), which are < 0.70. MgO (6.81-7.12 wt%), CaO (9.36-13.85 wt%) contents, and Mg# (56.6-62.5), indicate that these basalts represent slightly evolved volcanic products. These rocks have relatively high contents of TiO_2 (2.12-2.13 wt%)

and other incompatible elements, including P_2O_5 (0.33-0.36 wt%), Zr (171-162 ppm), Y (36-40 ppm), V (315-319 ppm), and Nb (10.7-13.2 ppm). They display generally high compatible element contents (Cr = 203-256 ppm, Ni = 60-74 ppm, Co = 39-40 ppm).

Incompatible element concentrations (Fig. 3c) show decreasing patterns from Th to Yb, as well as a mild enrichment in Th, U, Ta, Nb with respect to N-MORB. These elements range from ~5 to ~10 times N-MORB contents (Sun and McDonough, 1989). REE patterns (Fig. 3d) have LREE enrichment with respect to MREE and HREE, as exemplified by the La_N/Sm_N and La_N/Yb_N ratios, which are 1.47-1.79 and 2.71-3.23, respectively. The overall enrichments for LREE and HREE are of ~40-50 and ~15-17 times chondrite, respectively. In accordance with their relatively less evolved nature, no Eu negative anomalies are observed (Fig. 3d).

The HFSE and REE concentrations indicate that these rocks share affinities with enriched-type ocean-floor basalts (E-MORB). Accordingly, the Ti/V ratios (11-43) are typical values for basalts generated at mid-ocean ridge settings (Shervais, 1982), and in the Th-Ta-Hf/3 discrimination diagrams of Fig. 4 Group 2 basalts plot in the fields for E-MORB composition.

E-MORBs may originate either from low degree partial melting of depleted N-MORB type sub-oceanic mantle sources, or from slightly enriched mantle sources. Elemental ratios plotted in Fig. 5 indicate that these balsalts most likely represent melts derived from mantle sources somewhat influenced by an enriched OIB-type component. An estimation of the composition of primary magmas and relative mantle sources can be obtained using hygromagmatophile element ratios. These elements are weakly fractionated by fractional crystallization processes and, therefore, when used for primary or moderately fractionated rocks, hygromagmatophile element ratios are thought to represent the elemental ratios in the source (Allègre and Minster, 1978). The Th/Ta vs. Th/Tb ratios for the analyzed basalts are plotted in Fig. 6, where they show compositions quite distinct from N-MORB and OIB compositions. Elemental ratios
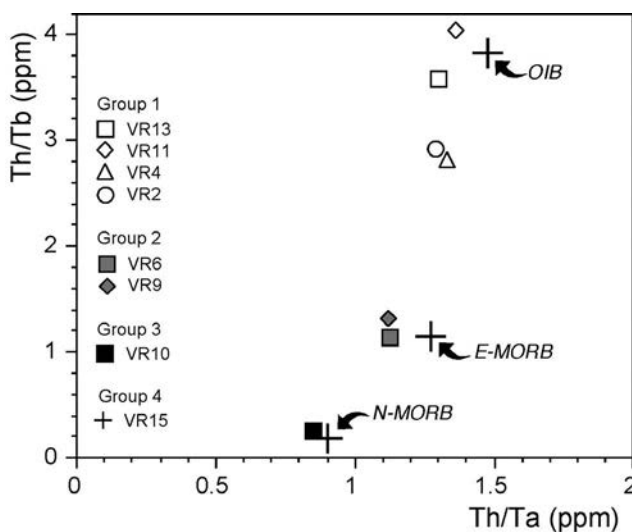

Fig. 6 - Th/Tb vs. Th/Ta diagram for Groups 1, 2, and 3 volcanic rocks from the mélange. Large crosses indicate the compositions of Modern ocean-island basalt (OIB), enriched-type mid-ocean ridge basalt (E-MORB), and normal-type mid-ocean ridge basalt (N-MORB), according to Sun and McDonough (1989).
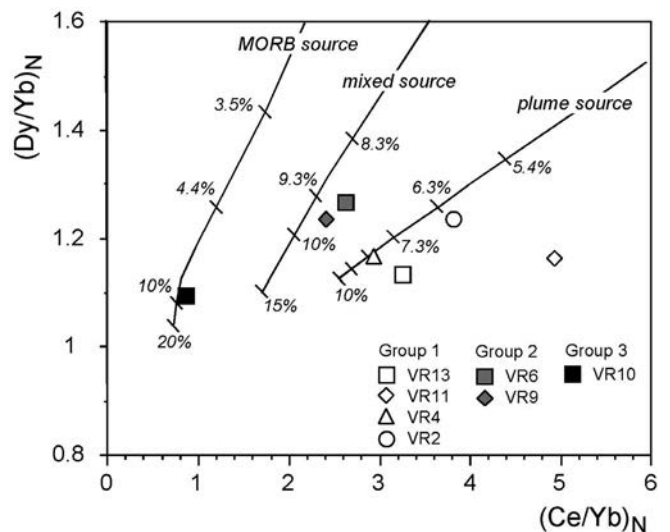

Fig. 7 - $(Dy/Yb)_N$ vs. $(Ce/Yb)_N$ diagram for Groups 1, 2, and 3 volcanic rocks from the mélange. Melt model is from Haase and Dewey (1996).

shown in Fig. 6 are generally compatible with a genesis from primary magmas originating from depleted N-MORB type sub-oceanic mantle sources influenced by enriched OIB-type material. This is also confirmed by the ratios of other highly incompatible trace elements as, for example, Ce/Y and La/Yb (Saunders et al., 1988) (Table 1). According to the model proposed by Haase and Devey (1996), their $(Dy/Yb)_N$ and $(Ce/Yb)_N$ compositions are compatible with ~9-10% partial melting of a theoretical mixed MORB-OIB mantle source (Fig. 7). In summary, the chemistry of Group 3 basalts points to generation in a mid-ocean ridge tectonic setting from a primitive MORB-type mantle source enriched by an OIB-type component. In addition, the E-MORBs studied in this paper display many similarities with E-MORBs from various localities of the Hellenides (Saccani et al., 2003b; Saccani and Photiades, 2005, and references therein), as shown in Fig. 5.

Group 3 (Normal-type mid-ocean ridge basalt).

Group 3 is represented by one basaltic sample (VR10) from outcrop 3 (Fig. 1). This basalt has a sub-alkaline nature, with very low Nb/Y ratio (Table 1). MgO (6.30 wt%), CaO (9.80 wt%) contents, and Mg# (55.4), indicate that this basalt represents a slightly evolved volcanic product. This rock is characterized by relatively high contents in TiO_2 (1.84 wt%) and other incompatible elements, including P_2O_5 (0.23 wt%), Zr (120 ppm), Y (35 ppm), V (304 ppm), coupled with low Nb (2.74 ppm), Th (0.20 ppm), Ta (0.24 ppm) and U (0.09 ppm). In agreement with its slightly evolved nature, this basalt has moderate contents of compatible elements (Cr = 136 ppm, Ni = 47 ppm, Co = 41 ppm).

The distribution of HFSE concentrations (Fig.3c) indicates that this rock shares affinity with normal-type ocean-floor basalts. In particular, elements from Th to Yb exhibit rather flat pattern, ranging from 1.0 to 1.5 times N-MORB contents (Sun and McDonough, 1989). The REE pattern (Fig. 3d) is consistent with a N-MORB composition, as it has mild LREE depletion ($La_N/Sm_N = 0.58$, $La_N/Yb_N = 0.75$) and an overall enrichment for HREE of ~10 times chondrite. In accordance with their slightly evolved nature, a modest Eu negative anomaly can be observed (Fig. 3d).

The Ti/V ratio of basalt VR10 (37) is in the range of typical values for basalts generated at mid-ocean ridge settings (Shervais, 1982). In the Th-Ta-Hf/3 discrimination diagrams of Fig. 4, Group 3 basalt plots in the field for N-MORB composition.

Elemental ratios plotted in Figs. 5 and 6 suggest that this basalt is compatible with a genesis from primary magmas originating from depleted N-MORB type sub-oceanic mantle sources, with no influence of enriched OIB-type material, as also confirmed by the low Ce/Y ratio (Table 1). According to the model proposed by Pearce (1983), the Cr and Y composition of Group 3 basalt is compatible with ~15% partial melting of a depleted MORB mantle source. Likewise, according to the model proposed by Haase and Devey (1996), their $(Dy/Yb)_N$ and $(Ce/Yb)_N$ compositions are compatible with ~10% partial melting of a depleted MORB mantle source (Fig. 7). In summary, the chemistry of Group 3 basalt points out to generation in a mid-ocean ridge tectonic setting from a primitive MORB-type mantle source.

Group 4 (Calc-alkaline rhyolite)

Group 4 is represented by rhyolite VR15 from outcrop 6. Its sub-alkaline affinity, is testified by the Nb/Y ratio = 0.30. As distinctive features, this rock has high SiO_2 content (72.52 wt%) and low MgO (3.34 wt%), TiO_2 (0.47 wt%), Al_2O_3 (11.69 wt%), Zr (77 ppm), and Y (25 ppm) contents. This rock is also characterized by very low Cr, Co, and Ni contents.

The incompatible element pattern (Fig. 3) is characterised by Th, La and Ce positive anomalies, and Ta, Nb, P, Ti negative anomalies. The chondrite-normalized REE pattern (Fig. 3d) is regularly decreasing from LREE to HREE and is characterized by significant LREE enrichment, with La_N/Sm_N and La_N/Yb_N ratios of 2.78 and 6.48, respectively. In addition, a marked negative Eu anomaly is observed.

The incompatible elements and REE abundance (Fig. 3c, d) exhibit patterns which are very similar to those of calc-alkaline rocks of the orogenic series (Pearce, 1983). Accordingly, in the discrimination diagrams shown in Fig. 4: the VR15 rhyolite, although it represents a very differentiated rock, plots in the field for calc-alkaline basalts.

The incompatible element and REE distribution of rhyolite VR15 (Fig. 3c, d) indicates that it is related to partial melting of a depleted mantle source further enriched by a subduction component. In particular, this subduction component is evident in the marked enrichment in Th with respect to Ta (Fig. 5). Fig. 5 also shows the close similarity between this rock and Triassic calc-alkaline and shoshonitic rocks from several localities in the Hellenides (Capedri et al., 1997; Pe-Piper, 1998; Pe-Piper and Piper, 2002, and references therein). These rocks are interpreted as having originated in a continental extensional setting from a mantle source bearing subduction-related geochemical characteristics inherited from a Hercynian subduction slab dipping below Gondwana (Pe-Piper, 1998). This extensional setting is associated with Permian-Triassic extension of the continental crust, which preceded the Vardar oceanic spreading. In lack of any other evidence, a similar tectono-magmatic environment of formation can reasonably be proposed also for Group 4 rhyolite studied in this paper.

BIOSTRATIGRAPHY

We collected 8 chert samples for radiolarian analyses. The samples have been etched with hydrochloric and hydrofluoric acid at different concentrations, using the method proposed by Dumitrica (1970) and Pessagno and Newport (1972).

In this chapter we report the radiolarian assemblages of each sample, the ages (resulted of a time span from Middle Triassic to Middle-Late Jurassic) and the stratigraphic distribution of the most important markers.

The preservation of the radiolarians was generally from poor to moderately, only one sample (VR16) yielded very well preserved radiolarians.

Middle Triassic (Plate 1: 1 - 9)

VR3 - *Baumgartneria bifurcata* Dumitrica, *Oertlispongus inaequispinosus* Dumitrica, Kozur and Mostler, *Paroertlispongus* sp. cf. *P. multispinosus* Kozur and Mostler.

The age of the sample is early Ladinian (upper part of *Spongosilicarmiger italicus* Zone) for the presence of *Baumgartneria bifurcata* Dumitrica and *Oertlispongus inaequispinosus* Dumitrica, Kozur and Mostler.

Range Taxa: *Baumgartneria bifurcata* Dumitrica, in Kozur and Mostler (1994) De Wever et al. (2001) (early Fassanian); *Oertlispongus inaequispinosus* Dumitrica, Kozur and Mostler in Kozur and Mostler (1994), Kozur and

Mostler (1996), De Wever et al. (2001) (early Fassanian-middle Longobardian).

After the definition of Anisian/Ladinian boundary, in Brack et al. (2005), the age of the sample VR3 could be late Illyrian (latest Anisian).

VR5 - *Paroertlispongus multispinosus* Kozur and Mostler.

The age of the sample is late Anisian-early Ladinian for the presence of *Paroertlispongus multispinosus* Kozur and Mostler.

<u>Range Taxon</u>: *Paroertlispongus multispinosus* Kozur and Mostler in Kozur and Mostler (1994), Kozur et al. (1996a) and Goriçan et al. (2005) (early Illyrian-early Fassanian).

After the definition of Anisian/Ladinian boundary, in Brack et al. (2005), the age of the sample VR5 could be late Anisian.

VR16 - *Archaeocenosphaera* sp. cf. *A. clathrata* (Parona), *Archaeocenosphaera* sp., *Eptingium manfredi* Dumitrica, *Pararchaeospongoprunum* sp. cf. *P. hermi* Lahm, *Paroertlispongus multispinosus* Kozur and Mostler, *Plafkerium* sp., *Tiborella florida* (Nakaseko and Nishimura), *Tiborella* sp.

The age of the sample is late Anisian (*Tetraspinocyrtis laevis* Zone and *Tiborella florida* subzone) for the presence of *Eptingium manfredi* Dumitrica, *Paroertlispongus multispinosus* Kozur and Mostler and *Tiborella florida* (Nakaseko and Nishimura).

<u>Range Taxa</u>: *Eptingium manfredi* Dumitrica, in Dumitrica (1978), Kozur and Mostler (1994), Goriçan et al. (2005) (late Anisian-early Ladinian); *Paroertlispongus multispinosus* Kozur and Mostler in Kozur and Mostler (1994), Kozur et al. (1996a) and Goriçan et al. (2005) (early Illyrian-early Fassanian); *Tiborella florida* (Nakaseko and Nishimura) in Kozur et al. (1996b) and Goriçan et al. (2005) (early-late Illyrian).

After the definition of Anisian/Ladinian boundary, in Brack et al. (2005), the age of the sample VR16 could be early Illyrian (late Anisian).

Late Triassic (Plate 1: 10 - 13)

VR7 - *Capnodoce anapetes* De Wever, *Capnodoce media* Blome, *Capnodoce* sp., *Capnuchosphaera concava* De Wever, *Capnuchosphaera* sp., *Spongotortilispinus tortilis* (Kozur and Mostler).

The age of the sample is latest Carnian-early Norian for the presence of *Capnodoce media* Blome and *Spongotortilispinus tortilis* (Kozur and Mostler).

<u>Range Taxa</u>: *Capnodoce anapetes* De Wever, in Tekin (1999) (late Carnian-late Norian); *Capnodoce media* Blome in Tekin (1999) (latest Carnian/earliest Norian-early Norian - ?late middle Norian); *Capnuchosphaera concava* De Wever in Tekin (1999) and Bragin (2007) (early Carnian-middle Norian); *Spongotortilispinus tortilis* (Kozur and Mostler) in Tekin (1999) and Bragin (2007) (late Ladinian-early Norian).

Middle-Late Jurassic (Plate 1: 14 - 21)

VR1 - *Arcanicapsa* sp. cf. *A. leiostraca* (Foreman); *Archaeodictyomitra* sp. cf. *A. patricki* Kocher, *Archaeodictyomitra* sp., *Archaeospongoprunum imlayi* Pessagno, *Archaeospongoprunum* sp., *Monotrabs goricanae* Beccaro, *Podobursa* sp., *Pseudodictyomitrella tuscanica* (Chiari, Cortese and Marcucci), *Protunuma* sp., *Saitoum pagei* Pessagno, *Tripocyclia smithi* Pessagno and Yang, *Zhamoidellum* sp.

The age of the sample is late Bathonian-early Callovian to middle Callovian-early Oxfordian for the presence of *Monotrabs goricanae* Beccaro, and *Pseudodictyomitrella tuscanica* (Chiari, Cortese and Marcucci).

<u>Range Taxon</u>: *Monotrabs goricanae* Beccaro in Beccaro (2004) (UAZ. 6-8); *Pseudodictyomitrella tuscanica* (Chiari, Cortese and Marcucci) in Chiari et al. (2007) (UAZ. 7-10).

VR12 - *Eucyrtidiellum unumaense* s.l. Yao, *Minocapsa* sp., *Unuma* sp., *Williriedellum* sp. cf. *W madstonenese* (Pessagno, Blome and Hull).

The age of the sample is early-middle Bajocian to middle Callovian-early Oxfordian for the presence of *Eucyrtidiellum unumaense* s.l. (Yao).

<u>Range Taxon</u>: *Eucyrtidiellum unumaense* s.l. (Yao) in Baumgartner et al. (1995) (UAZ. 3-8).

DISCUSSION AND CONCLUSIONS

From our data it is possible to infer some intriguing conclusions about the geologic evolution of the area during Eocenic times.

The data collected for this work attest that the elements included in the studied mélange have the same compositions of the ones from the widespread Subophiolitic Mélange that lies below the main ophiolitic massifs of the Hellenides and/or at the top of the Adria-derived tectonic units. In fact, it includes continent-derived and ocean-derived blocks, the latter comprising Triassic and Jurassic WP, E-MOR and N-MOR basalts. As the ophiolite lithic fragments in the sandstone of the Pindos Flysch (Gonzales-Bonorino, 1996), the ophiolite bearing debris flow deposits and slide blocks had a source area to the east, from the advancing Ophiolite Nappe (with at its base the Subophiolitic Mélange).

The ophiolite mass flow deposits included in the upper portion of the Flysch date to the Eocene the age of the westward thrusting of the Ophiolite Nappe into the Pindos Flysch Basin. The Pindos Basin represents the westernmost position reached by the Ophiolite Nappe in its long thrust journey: some hundred kms in more than 100 ma. Remnants of the Subophiolitic Mélange are preserved as *klippen* above the Eocene Parnassus Flysch and Pelagonian limestones in the Iti Mt. and, more to the SE, in Kallidromon Mt., above the same Pelagonian limestones, (Karipi et al., 2008). From the Late Eocene, the thrusting of the Parnassus Unit onto the Pindos Basin (Celet, 1962) and then the activation of westward propagating thrusts on the Pindos Unit (Skourlis and Doutsos, 2003) deactivated the sole thrust of the Internal Hellenides. After these events the Ophiolite Nappe moved westwards only passively on top of the Adria-derived units.

According to Degnan and Robertson (1993) the oceanic basin between Adria and the Parnassus Microcontinent was consumed through an east-dipping intraoceanic subduction. Following this hypothesis the ophiolitic units would be expected to be accreted together with the Pindos Flysch and to be interposed between the Parnassus/Vardoussia Units and the Pindos Basin. As matter of fact, no evidence of tectonic slices in this structural position is found in Etolia and all along the Hellenic chain. As observed also in other areas (Principi et al., 2008), the oceanic and continental crust-derived mass flow deposits in the Pindos Flysch of eastern Etolia represent the precursors of the westward tectonic emplacement of the Ophiolite Nappe+Subophiolitic Mélange onto the Pindos Basin.

The sampled rhyolite, like those found in several localities of the Hellenides, testifies an extensional phase in the continental crust of the Pindos Basin during the Middle Triassic (Pe-Piper and Piper, 2002). It has an unclear tectonic setting: it can be interpreted, as proposed by Skourlis and Doutsos (2003), as a tectonic slice interposed in the Flysch with a duplex geometry or, alternatively, as a slide block included in the Pindos Flysch. In any case, this mass indicates that an intracontinental Tertiary compressional phase (Mesohellenic stage, Jacobshagen, 1986) involved the Pindos Basin.

Concluding, no evidences of an oceanic basin related with the Pindos Unit can be found in the east Etolia area. As a matter of facts, all along the Pindos Unit in Greece as well as in its continuation in Albania (Cukali Unit), no evidences for the existence of a Mesozoic oceanic basin between the Internal and External Dinarides could be found (see Bortolotti et al., 2004; Bortolotti and Principi, 2005). The intercalations of ophiolitic and continent-derived material in the Pindos Flysch, are interpreted as the forerunners of the Ophiolite Nappe which, coming from the Vardar Ocean to the east, reaches during the Eocene the Pindos Basin.

ACKNOWLEDGMENTS

REFERENCES

Alexander J., Nichols G.J. and Leigh S., 1990. The origins of marine conglomerates in the Pindus foreland basin, Greece. Sedim. Geol., 66: 243-54.

Allègre C.J. and Minster J.F., 1978. Quantitative models of trace element behavior in magmatic processes. Earth Planet. Sci. Letters, 38: 1-25.

Baumgartner P.O., O'Dogherty L., Goriçan S., Dumitrica-Jud R., Dumitrica P., Pillevuit A., Urquhart E., Matsuoka A., Danelian T., Bartolini A.C., Carter E.S., De Wever P., Kito N., Marcucci M. and Steiger T.A., 1995. Radiolarian catalogue and systematics of Middle Jurassic to Early Cretaceous Tethyan genera and species. In: P.O. Baumgartner et al. (Eds.), Middle Jurassic to Lower Cretaceous Radiolaria of Tethys: occurrences, systematics, biochronology. Mém. Géol., Lausanne, 23: 37-685.

Beccaro P., 2004. *Monotrabs goricanae* n. sp.: a new species of Jurassic Tritrabidae (spumellarian Radiolaria). Micropal., 50 (1): 81-87.

Beck C., 1975. Etude géologique des formations allochtones du synclinorium Est-Etolique (Grèce Continentale). PhD Thesis, Univ. Sci. Technol. Lille, 123 pp.

Beck C.M., 1980. Essai d'interpretation structurale et paléogéographique des roches vertes du Pinde d'Etolie (Grèce continental méridionale). Ann. Soc. Géol. Nord, 99: 355-365.

Bortolotti V., Chiari M., Marcucci M., Marroni M., Pandolfi L., Principi G. and Saccani E., 2004. Comparison among the Albanian and Greek ophiolites, in search of constraints for the evolution of the Mesozoic Tethys ocean. Ofioliti 29:19-35.

Bortolotti V., Chiari M., Marcucci M., Photiades A., Principi G. and Saccani E., 2008. New geochemical and age data on the ophiolites from the Othrys area (Greece): Implication for the Triassic evolution of the Vardar Ocean. Ofioliti, 33: 135-151.

Bortolotti V. and Principi G., 2005. Tethyan ophiolites and Panges break-up. Isl. Arc., 14: 442-470.

Bragin N.Y., 2007. Late Triassic radiolarians of southern Cyprus. Paleont. J., 41 (10): 951-1029.

Brack P., Rieber H., Nicora A. and Mundil R., 2005. The Global boundary Stratotype section and Point (GSSP) of the Ladinian Stage (Middle Triassic) at Bagolino (Southern Alps, Northern Italy) and its implications for the Triassic time scale. Episodes 28 (4): 233-244.

British Petroleum Co Ltd., 1971. The geological results of petroleum exploration in western Greece. Inst. Geol. Subsurf. Res., Spec. Rep. Athens, 10.

Capedri S., Toscani L., Grandi R., Venturelli G. Papanikolaou D. and Skarpelis N., 1997. Triassic volcanic rocks of some type-localities from the Hellenides. Chem. Erde, 57: 257-276.

Celet P., 1962. Contribution à l'étude géologique du Parnasse-Kiona et d'une partie des regions méridionales de la Grèce continentale. Ann. Géol. Pays Héllén., 13: 1-446.

Celet P., 1976. À propos du mélange de type "volcano-sédimentaire" de l'Iti (Grèce méridionale). Bull. Soc. Géol. France, 18: 299-307.

Celet P., 1977. Les bordures de la zone du Parnasse (Grèce). In: G. Kallergis (Ed.), Evolution paléogéographique au Mésozoîque et caractères structuraux. Proceed. VI Coll. Geol Aegean Region. I.G.M.E., Athens, 2: 725-740.

Chiari M., Cobianchi M. and Picotti V., 2007. Integrated biostratigraphy of Jurassic successions in the Southern Alps. Palaeo., Palaeo., Palaeo., 249: 233-270.

Degnan P. J. and Robertson A.H.F., 1998. Mesozoic-Early Tertiary passive margin evolution of the Pindos Ocean (NW Peloponnese, Greece). Sedim. Geol., 117: 33-70.

De Wever P., Dumitrica P., Caulet J.P., Nigrini C. and Caridrot M., 2001. Radiolarians in the sedimentary record. Gordon and Breach Science Publ., 533 pp.

Dickinson W.R. and Suczek C.A., 1979. Plate tectonics and sandstone compositions. AAPG Bull., 63: 2164-2182.

Dumitrica P., 1970. Cryptocephalic and cryptothoracic Nassellaria in some Mesozoic deposits of Romania. Rev. Roum. Géol., Géophys. Géogr., série Géol., 14 (1): 45-124.

Dumitrica P., 1978. Family Eptingidae n. fam., ext. Nassellaria (Radiolaria) with sagittal ring. Dari Seama, Inst. Geol. Geofiz., Bucureşti, 64: 57-74.

Faupl P., Pavlopoulos A. and Migiros G., 1999. The Paleogene history of the Pelagonian zone S.L. (Hellenides, Greece): Heavy mineral study from terrigenous flysch sediments. Geol. Carpathica, 50: 449-458.

Faupl P., Pavlopoulos A. and Migiros G., 2002. Provenance of the Peloponnese (Greece) flysch based on heavy minerals. Geol. Mag., 139: 513-524.

Frey F.A. and Clague D.A., 1983. Geochemistry of diverse basalt types from Loihi seamount, Hawaii. Earth Planet. Sci. Lett., 66: 337-355.

González-Bonorino G., 1996. Foreland sedimentation and plate interaction during closure of the Tethys Ocean (Tertiary; Hellenides; western continental Greece). J. Sedim. Res., 66: 1148-1155.

Goriçan Ş., Halamić J., Grgasović T. and Kolar-Jurkovšek T., 2005. Stratigraphic evolution of Triassic arc-backarc system in northwestern Croatia. Bull. Soc. Géol. France, 176 (1): 3-22.

Haase K.M. and Devey C.W., 1996. Geochemistry of lavas from the Ahu and Tupa volcanic fields, Easter hotspot, southeast Pacific: implications for intraplate magma genesis near a spreading axis. Earth Planet. Sci. Lett., 137: 129-143.

Jacobshagen V., 1986. Geologie von Griechenland. Borntraeger, Berlin Stuttgart, 363 pp.

Jones G. and Robertson A.H.F., 1991. Tectono-stratigraphy and evolution of the Mesozoic Pindos ophiolite and related units, northwestern Greece. J. Geol. Soc. London, 148: 267-288.

Karipi S., Tsikouras B., Pomonis P. and Hatzipanagiotou K., 2008. Geological evolution of the Iti and Kallidromon Mountains (central Greece), focused on the ophiolitic outcrops. Zeitsch. Deuts. Gesell. Geowiss., 159: 549-563.

Kozur H.W., Kaya O. and Mostler H., 1996a. First evidence of Lower to Middle Scythian (Dienerian-Lower Olenekian) radio-

larians from The Karakaya Zone of Northwestern Turkey. Geol. Paläont. Mitt. Innsbruck, Sond. 4: S. 271-285.

Kozur H.W., Krainer K. and Mostler H., 1996b. Radiolarians and Facies of the Middle Triassic Loibl Formation, South Alpine Karawanken Mountains (Carinthia, Austria). Geol. Paläont. Mitt. Innsbruck, Sond. 4: S. 195-269.

Kozur H.W and Mostler H., 1994. Anisian to middle Carnian radiolarian zonation and description of some stratigraphically important radiolarians. Geol. Paläont. Mitt. Innsbruck, Sond. S. 3: 39-255.

Kozur H.W. and Mostler H., 1996. Longobardian (late Ladinian) Oertlispongidae (Radiolaria) from the Republic of Bosnia-Hercegovina and the stratigraphic value of advanced Oertlispongidae. Geol. Paläont. Mitt. Innsbruck, Sonderband S. 11: 105-193.

Lachance G.R. and Trail R.J., 1966. Practical solution to the matrix problem in X-ray analysis. Can. Spectr., 11: 43-48.

Leigh S.P., 1991. The sedimentary evolution of the Pindos foreland basin, western Greece. Phd. Thesis, Univ. Wales, Cardiff, 181 pp.

Lipman P.W., Clague D.A., Moore J.G. and Holcomb R.T., 1989. South Arch volcanic field - Newly identified young lava flows on the sea floor south of the Hawaiian Ridge. Geology, 17: 611-614.

Neumann P., Risch H., Zacher W. and Fytrolakis N., 1996. Die stratigraphische und sedimentologische Entwicklung der Olonos-Pindos-Serie zwischen Koroni und Finikounda (SW-Messenien). N. Jb. Geol. Paläont., Abh., 200: 405-424.

Nirta G., Vannucchi P., Menna F., Chiari M., Principi G. and Saccani E., 2009. The emplacement of the ophiolitic nappe onto continental crust: stratigraphic and structural evidences from the Pindos and Grammos areas (Nortern Greece). Geoitalia 2009, Rimini settembre 2009. Epitome, 3: 197-198.

Pearce J.A., 1983. Role of the sub-continenetal lithosphere in magma genesis at active continental margin. In: C.J. Hawkesworth and M.J. Norry (Eds.), Continental basalts and mantle xenoliths. Shiva Publ. Co., Nantwich: p. 230-249.

Pearce J.A. and Norry M.J., 1979. Petrogenetic implications of Ti, Zr, Y, and Nb variations in volcanic rocks. Contrib. Mineral. Petrol., 69: 33-47.

Pe-Piper G., 1998. The nature of Triassic extension-related magmatism in Greece: Evidence from Nd and Pb isotope geochemistry. Geol. Mag., 135: 331-348.

Pe-Piper G. and Hatzipanagiotou K., 1993. Ophiolitic rocks of the Kerassies-Milia belt, continental Greece. Ofioliti, 18 (2): 157-170.

Pe-Piper G. and Piper D.J.W., 2002. The igneous rocks of Greece. The anatomy of an orogen. Gebruder Borntraeger, Berlin: 573 pp.

Pessagno E.A. and Newport L.A., 1972. A technique for extracting Radiolaria from radiolarian chert. Micropal., 18 (2): 231-234.

Piper D.J.W., Panagos A.G. and Pe G., 1978. Conglomeratic Miocene flysch, western Greece. J. Sedim. Petr., 48: 117-26.

Principi G., Garfagnoli F., Menna F., Nirta G., Photiades A., Vannucchi P. and Saccani E., 2008. The Hellenic Internal Units of Grammos area (Northern Greece): preliminary data. Rend. Soc. Geol. It., 6: 140-142.

Richter D., Mariolakos I. and Risch H., 1978. The main flysch stages of the Hellenides. In: H. Closs, H.D. Roeder and K. Schmidt (Eds.), Alps, Apennines, Hellenides. E. Schweiz. Verlags. Handl., 38: 434-438.

Richter D. and Müller C., 1993. Die Flysch-Zonen Griechenlands VI. Zur Stratigraphie des Flysches der Pindos-Zone zwischen der Querzone von Kastaniotikos und dem Südpeloponnes (Griechenland). N. P. Geol. Paleont. Monatsch, 19: 449-476.

Robertson A.H.F, Clift P.D., Degnan P.J. and Jones G., 1991. Palaeogeographic and palaeotectonic evolution of the eastern Mediterranean Neotethys. Palaeo. Palaeo. Palaeo., 87: 289-343.

Robertson A.H.F. and Degnan P.J., 1993. Kerassia-Milia Complex: Evidence of a Mesozoic-Early Tertiary oceanic basin between the Apulian continental margin and the Parnassus carbonate platform in western Greece. Boll. Soc. Geol. Greece, 28: 233-246.

Saccani E., Padoa E. and Photiades A., 2003a. Triassic mid-ocean ridge basalts from the Argolis Peninsula (Greece): New constraints for the early oceanization phases of the Neo-Tethyan Pindos basin. In: Y. Dilek and P.T. Robinson (Eds), Ophiolites in Earth history, Geol. Soc. London Spec. Publ., 218: 1-19.

Saccani E. and Photiades A., 2005. Petrogenesis and tectono-magmatic significance of volcanic and subvolcanic rocks in the Albanide-Hellenide ophiolitic mélanges. In: Y. Dilek, Y. Ogawa, V. Bortolotti and P. Spadea (Eds.), Evolution of ophiolites in convergent and divergent plate boundaries, Isl. Arc, 14: 494-516.

Saccani E., Photiades A. and Padoa E., 2003b. Geochemistry, petrogenesis and tectono-magmatic significance of volcanic and subvolcanic rocks from the Koziakas Mélange (Western Thessaly, Greece). Ofioliti, 28: 43-57.

Saccani E., Photiades A., Santato A. and Zeda O., 2008. New evidence for supra-subduction zone ophiolites in the Vardar zone from the Vermion massif (northern Greece): Implication for the tectono-magmatic evolution of the Vardar oceanic basin. Ofioliti, 33: 65-85.

Saunders A.D., Norry M.J. and Tarney J., 1988. Origin of MORB and chemically-depleted mantle reservoirs: Trace element constraints. In: M.A. Menzies and K.G. Cox (Eds.), Oceanic and continental lithosphere: Similarities and differences. J. Petrol., Spec. Vol.: 414-445.

Shervais J.W., 1982. Ti-V plots and the petrogenesis of modern ophiolitic lavas. Earth Planet. Sci. Lett., 59: 101-118.

Skourlis K. and Doutsos T., 2003. The Pindos fold-and thrust belt (Greece): inversion kinematics of a passive continental margin. Int. J. Earth Sci., 92: 891-903.

Sun S.-S. and McDonough W.F., 1989. Chemical and isotopic-systematics of oceanic basalts: implications for mantle composition and processes. In: A.D. Saunders and M.J. Norry (Eds.), Magmatism in the ocean basins. Geol. Soc. London Spec. Publ., 42: 313-345.

Tekin U.K., 1999. Biostratigraphy and systematics of Late Middle to Late Triassic radiolarians from the Taurus Mountains and Ankara region, Turkey. Geol. Paläont. Mitt. Innsbruck, Sond. S. 5: 1-296.

Vakalas I., Ananiadis G., Zelilidis A., Kontopoulos N. and Tsikouras B., 2004. Provenance of Pindos foreland flysch deposits using scanning electron microscopy and microanalysis. Proceed. 10th Intern. Congr., Thessaloniki, 2004, Bull. Geol. Soc. Greece, 36: 607-614.

Wood D.A., 1980. The application of a Th-Hf-Ta diagram to problems of tectonomagmatic classification and to establishing the nature of crustal contamination of basaltic lavas of the British Tertiary volcanic province. Earth Planet. Sci. Lett., 50: 11-30.
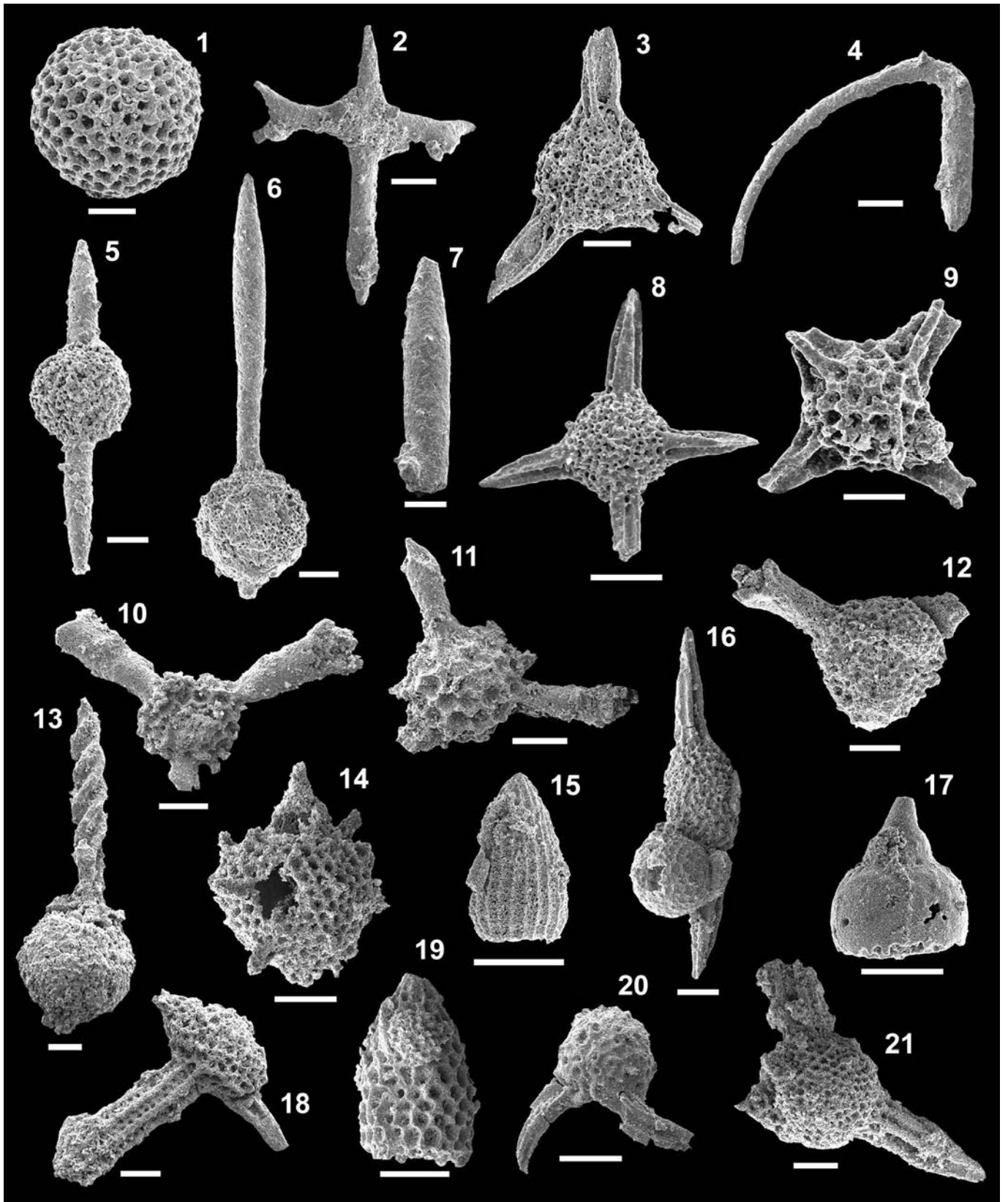
Plate 1 <u>Middle Triassic.</u> **1)** *Archaeocenosphaera* sp. cf. *A. clathrata* (Parona), VR16; **2)** *Baumgartneria bifurcata* Dumitrica, VR3; **3)** *Eptingium manfredi* Dumitrica, VR16; **4)** *Oertlispongus inaequispinosus* Dumitrica, Kozur and Mostler, VR3; **5)** *Pararchaeospongoprunum* sp. cf. *P. hermi* Lahm, VR16; **6)** *Paroertlispongus multispinosus* Kozur and Mostler, VR16; **7)** *Paroertlispongus multispinosus* Kozur and Mostler, VR5; **8)** *Plafkerium* sp., VR16 **9)** *Tiborella florida* (Nakaseko and Nishimura), VR16.

<u>Late Triassic</u>. **10)** *Capnodoce anapetes* De Wever, VR7; **11)** *Capnodoce media* Blome, VR7; **12)** *Capnuchosphaera concava* De Wever, VR7; **13)** *Spongotortilispinus tortilis* (Kozur and Mostler); VR7.

<u>Middle-Late Jurassic</u>. **14)** *Arcanicapsa* sp. cf. *A. leiostraca* (Foreman), VR 1; **15)** *Archaeodictyomitra* sp. cf. *A. patricki* Kocher, VR1; **16)** *Archaeospongoprunum imlayi* Pessagno, VR1; **17)** *Eucyrtidiellum unumaense* s.l. Yao, VR 12; **18)** *Monotrabs goricanae* Beccaro, VR1; **19)** *Pseudodictyomitrella tuscanica* (Chiari, Cortese and Marcucci), VR1; **20)** *Saitoum pagei* Pessagno, VR1; **21)** *Tripocyclia smithi* Pessagno and Yang, VR1.
Scale bar=50μ.